

CO₂-Involved and Isocyanide-based Three-component Polymerization toward Functional Heterocyclic Polymers with Self-assembly and Sensing Properties

Dongming Liu,[†] Bo Song,[†] Jia Wang,[†] Baoxi Li,[†] Bingnan Wang,[†] Mingzhao Li,[†] Anjun Qin,^{†} Ben Zhong Tang^{*†,‡}*

[†] State Key Laboratory of Luminescent Materials and Devices, Guangdong Provincial Key Laboratory of Luminescence from Molecular Aggregates, SCUT-HKUST Joint Research Institute, AIE Institute, Center for Aggregation-Induced Emission, South China University of Technology (SCUT), Guangzhou 510640, China. E-mail: msqinaj@scut.edu.cn

[‡] Department of Chemistry, Hong Kong Branch of Chinese National Engineering Research Center for Tissue Restoration and Reconstruction, Institute for Advanced Study, and Department of Chemical and Biological Engineering, The Hong Kong University of Science & Technology (HKUST), Hong Kong, Kowloon, Hong Kong 999077, China

ABSTRACT: CO₂ utilization has been a hot research topic in academic and industrial respects. Besides converting CO₂ into chemicals and fuels, incorporating it into the polymers to construct functional materials is another promising strategy. However, the CO₂-involved polymerization techniques should be further developed. In this work, a facile and efficient CO₂-involved multicomponent polymerization is successfully developed. The reaction of monomers of CO₂, isocyanides and 2-iodoanilines readily produces soluble and thermally stable poly(benzoyleneurea)s with well-defined structures under mild conditions. Thanks to the formed amide groups in the heterocyclic units in the main-chains, the resultant polymers could self-assemble into spheres with sizes between 200 and 1000 nm. The polymers containing tetraphenylethylene (TPE) unit show the unique aggregation-enhanced emission (AEE) features, which could be used to visualize the self-assembly process and morphologies under UV irradiation, and serve as fluorescence probe to selectively and sensitively detect Au³⁺ ions. Notably, the polymers containing *cis*- and *trans*-TPE units exhibit different behaviors in self-assembly and limit of detection for Au³⁺ ions due to the different intermolecular interactions. Thus, this work not only provides a new strategy for CO₂ utilization but also furnishes a series of functional heterocyclic polymers for diverse applications.

Introduction

In the past decades, the conversion and utilization of abundant, non-toxic and renewable carbon dioxide (CO₂) have become a hot topic in both academic and industrial respects.¹⁻⁶ Although CO₂ possesses thermodynamic stability and kinetic inertness, a large number of works on converting CO₂ into chemicals and fuels via the constructions of C-O, C-N, C-C and C-H bonds have been reported.⁷⁻¹⁰ Meanwhile, the transformation of CO₂ into functional polymers is receiving considerable attentions in polymer chemistry. However, most of the reports are mainly focused on the preparation of chain polymers.¹¹⁻¹⁹ It is very challenging to synthesize heterocyclic polymers by the CO₂-involved polymerization.

Generally, the preparation of heterocyclic polymers from CO₂-involved polymerizations can be achieved via following two strategies: (1) firstly transforming CO₂ into monomers, such as 3-ethylidene-6-vinyltetrahydro-2H-pyran-2-one (EVL)²⁰⁻²² and five-membered cyclic carbonates (5CC)s,^{23,24} (2) directly using CO₂ as a monomer. The latter is preferred and elegant works have been done. For example, Tsuda and coworkers reported a nickel complex-catalyzed alternating copolymerization of CO₂ and diynes towards poly(2-pyrone)s.^{25,26} However, the copolymerization was carried out under high pressure (20-50 bar). In 2012, Li and coworkers developed a multi-component polycoupling of benzaldehyde, 1,4-diethynylbenzene, 1,6-hexadiazine and CO₂.²⁷ However, the resultant polyoxazolidinones showed poor solubility, which hinders their further properties study and application exploration. In 2018, Dong and coworkers reported a catalyst-free multicomponent spiropolymerization of diisocyanides, alkynes and CO₂ and soluble spiropolymers were successfully obtained.²⁸ Our group also developed a three-component polymerization of CO₂, bis(propargylic alcohol)s, and aryl dihalides under atmospheric pressure recently.²⁹ Nevertheless, these polymerizations could only obtain oxygen-containing heterocyclic

polymers. Therefore, we anticipate that distinctive monomers, such as isocyanides can be incorporated in CO₂-involved polymerizations under mild reaction conditions towards novel heterocyclic polymers.

Isocyanides have been widely used to construct heterocycles.^{30,31} Thanks to the widespread applications of isocyanides in multicomponent reactions (MCRs),³²⁻³⁴ and according to the reported works,³⁵⁻³⁷ we hypothesized that a novel multi-component polymerization (MCP) based on the monomers of CO₂ and isocyanides could be established under mild reaction conditions, from which heterocyclic polymers could be readily generated and unique properties should be found. Indeed, after a systematical investigation, a MCP of CO₂, diisocyanides and bis(2-iodoaniline)s was developed and a series of poly(benzoyleneurea)s with well-defined structures were constructed. Notably, the resultant polymers could self-assemble into solid spheres and the polymers bearing tetraphenylethene (TPE) moieties showed the unique aggregation-enhanced emission (AEE) characteristic, which could be used as a fluorescence probe to sensitively detect Au³⁺ ions.

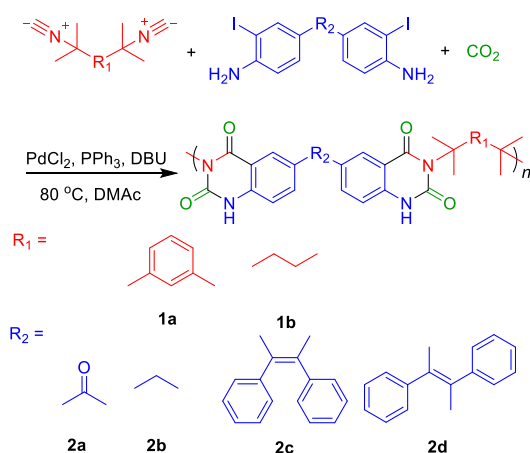
Results and Discussion

Monomers Synthesis. Diisocyanides **1a** and **1b** (Scheme S1 and S2) were prepared according to the synthetic procedures given in literature.³⁸⁻⁴⁰ Inspired by the preparation method of 2-iodoaniline,^{41,42} bis(2-iodoaniline)s **2a-2d** (Scheme S3 and S4) were prepared for the first time as far as we know.

Model Reaction. Before exploration of the CO₂ involved and isocyanide-based polymerization, the model reaction was carried out using 2-iodoanilines, *tert*-butyl isocyanide and CO₂ as the reactants following the reported procedures (Scheme S5).³⁶ The three-component reaction proceeded smoothly in the presence of catalytic system of PbCl₂, PPh₃ and 1,8-

diazabicyclo[5.4.0]undec-7-ene (DBU) in *N,N*-dimethylacetamide (DMAc) under atmospheric pressure CO₂, which generated a model compound **3** in 90% yield. The structure of **3** was characterized by FT-IR (Figure 1C), ¹H and ¹³C NMR (Figure 2C and 3C) spectroscopies and satisfactory results were obtained.

Polymerization. Encouraged by the positive results of above highly efficient model reaction, we set out to develop relevant MCP (Scheme 1). Herein, **1a** and **2a** were chosen as representative monomers to systematically investigate the polymerization conditions.



Scheme 1. Multi-Component Polymerization of CO₂, Diisocyanides, and Bis(2-iodoaniline)s in the Presence of PdCl₂, PPh₃ and DBU under Atmosphere Pressure.

First, we investigated the effect of solvents on the polymerization. Among the used solvents of tetrahydrofuran (THF), toluene, acetonitrile, 1,2-dichloroethane (DCE), dimethyl sulfoxide (DMSO), *N,N*-dimethylformamide (DMF) and DMAc, a superior polymerization result was obtained in DMAc, furnishing a soluble polymer with the weight-average molecular weight (*M_w*) of 6500 in a 82% yield (Table S1). The results suggest that high polarity solvents could favor this polymerization because they can well dissolve the resultant products.

Second, we studied the effect of catalysts and the base loading on the polymerization. Among the testing catalysts, PdCl₂/PPh₃ was the most efficient one (Table S2), and the highest catalytic

activity for this polymerization was showed in the presence of 15 mol% of PdCl₂ and 30 mol% of PPh₃ (Table S3). Notably, the base loading plays a significant role in the polymerization. A poor result was obtained when the amount of base decreased from 3 to 2 equiv. of monomers (Table S4, entry 1). Hence, 15 mol% of PdCl₂, 30 mol% of PPh₃ and 3 equiv. of DBU were chosen for following polymerizations.

Third, the effect of temperature on the polymerization was explored. As depicted in Table S5, the results showed that the polymer with a higher M_w was obtained in a 83% yield at 80 °C (Table S5, entry 2). By increasing the polymerization temperature to 90 °C, no obvious increment in the M_w and yield was observed. We thus considered 80 °C as the optimal polymerization temperature.

Forth, we tested the effect of monomer concentrations on the polymerization, and the results are shown in Table S6. It was found that the M_w values and yields of resultant polymers enhanced first and then decreased when concentration of **1a** increased from 0.05 to 0.4 M. Taking the yield and M_w into the consideration, we referred 0.1 M as the best monomers concentration.

Finally, we systematically screened the time course on the polymerization (Table S7). The yield and M_w of the resultant polymers gradually increased with the extension of polymerization time and reached the maximum of 86% and 8700 at 18 h, respectively. Further prolonging the reaction time to 24 h led to a slight decline in the yield of the product. Therefore, we used 18 h as the reaction time.

With these optimal polymerization conditions in hand, we polymerized different bis(tertiary isocyanide)s **1** and bis(2-iodoaniline)s **2** monomers under atmospheric pressure CO₂ to verify its robustness and universality. The results showed that all the polymerizations proceed smoothly, furnishing corresponding polymers with acceptable M_w values (up to 8700) in satisfactory yields (up to 86%) (Table 1).

Table 1. Polymerization Results of Bis(tertiary isocyanide)s **1** and Bis(2-iodoaniline)s **2** and CO₂.^a

entry	monomer	polymer	yield (%)	M_w^b	D^b
1	1a + 2a + CO ₂	P 1a/2a /CO ₂	86	8700	1.82
2	1a + 2b + CO ₂	P 1a/2b /CO ₂	80	7500	1.74
3	1a + 2c + CO ₂	P 1a/2c /CO ₂	73	6700	1.56
4	1a + 2d + CO ₂	P 1a/2d /CO ₂	84	7100	1.69
5	1b + 2a + CO ₂	P 1b/2a /CO ₂	64	7700	1.63
6	1b + 2b + CO ₂	P 1b/2b /CO ₂	69	5600	1.43
7	1b + 2c + CO ₂	P 1b/2c /CO ₂	54	6000	1.45
8	1b + 2d + CO ₂	P 1b/2d /CO ₂	60	6300	1.48

^aCarried out in DMAc at 80 °C under atmosphere CO₂ (balloon) for 18 h in the presence of PdCl₂, PPh₃ and DBU. [1] = 0.10 M. [1]/[2]/[PbCl₂]/[PPh₃]/[DBU] = 1:1:0.15:0.3:3. ^bEstimated by GPC with DMF containing 0.05 M LiBr as an eluent on the basis of a linear polymethyl methacrylate (PMMA) calibration; D = polydispersity index (M_w/M_n , M_w = Weight-average Molecular Weight, M_n = Number-average Molecular Weight).

Due to the strong hydrogen bonds of formed amide groups, the resultant polymers showed poor solubility in less polar solvents, such as THF, DCM, but were fully soluble in highly polar organic solvents of DMAc, DMF, DMSO and 1,1,1,3,3,3-hexafluoro-2-propanol (HFIP), *etc.* They also exhibited good thermal stability. The experimental results of thermogravimetric analysis (TGA) measurement reveal that the temperatures for 5% weight loss (T_d) of the polymers are in the range of 205–246 °C (Figure S1).

Structural Characterization. To obtain the structural information of resultant polymers, FT-IR and NMR spectroscopy measurements were carried out. Since P**1a/2b**/CO₂ could provide more characteristic structural information, we thus selected it as a representative example for the discussion of the structural characterization.

In the FT-IR spectra (Figure 1), the strong stretching vibration of $-\text{N}^+\equiv\text{C}^-$ in **1a** appeared at 2143 cm^{-1} , whereas, that of the $-\text{NH}_2$ in **2b** was observed at 3436 and 3326 cm^{-1} . In the spectra of model compound **3** and **P1a/2b/CO₂**, these peaks were hardly observed, which indicated that monomers were consumed. Meanwhile, new peaks of $-\text{NH}$ in the spectra of **3** and **P1a/2b/CO₂** were emerged at 3204 and 3275 cm^{-1} , respectively, and new peaks assigned to the two $\text{C}=\text{O}$ in structure of benzoyleneurea appeared at 1715 and 1671 cm^{-1} . These results indicate that the MCP of CO_2 , isocyanides and 2-iodoanilines proceeded well.

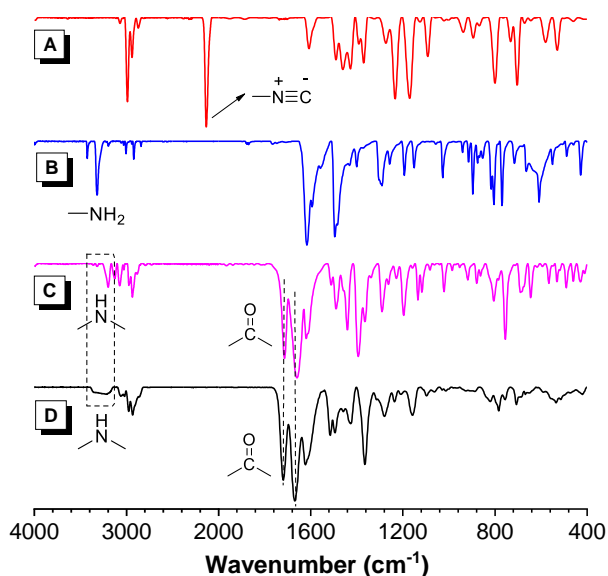


Figure 1. FT-IR spectra of (A) isocyanide **1a**, (B) 2-iodoanilines **2b**, (C) model compound **3**, and (D) **P1a/2b/CO₂**.

More detailed information of the polymer structures can be acquired from the NMR spectra. As shown in Figure 2, in the ^1H NMR spectra, the resonances of methyl proton in **1a** and methylene one in **2b** remained in the model compound **3** and **P1a/2b/CO₂**. However, primary amine protons of **2b** at δ 5.01 were almost absent in the spectra of **3** and **P1a/2b/CO₂**, indicating that **2b** had been

almost completely consumed. Meanwhile, new peaks at δ 11.01 and 10.8 in the spectra of **3** and **P1a/2b/CO₂** could be ascribed to the resonance of the amidic protons of benzoyleneurea units.

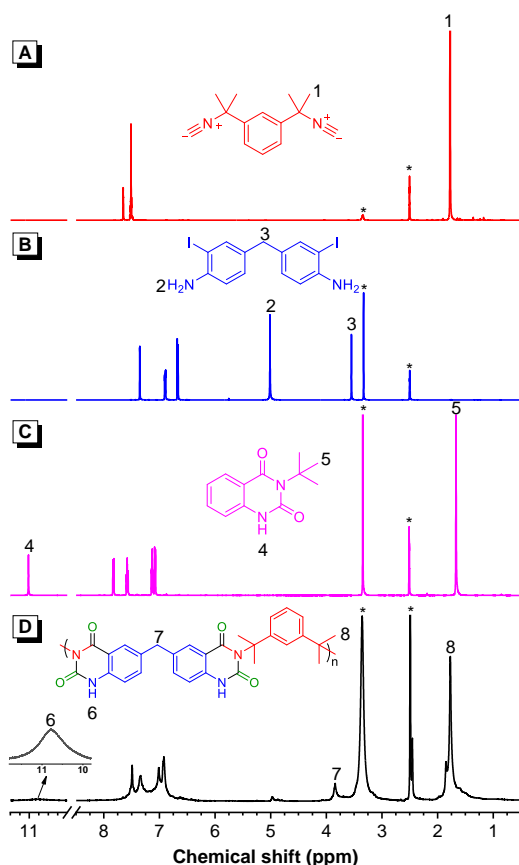


Figure 2. ¹H NMR spectra of (A) monomer **1a**, (B) monomer **2b**, (C) model compounds **3**, and (D) **P1a/2b/CO₂** in DMSO-*d*₆. The solvent peaks are marked with asterisks.

The ¹³C NMR analysis further confirms the polymer structures. As shown in Figure 3, the characteristic carbons of isocyanide groups in **1a** and those adjacent to the iodine groups in **2b** resonated at δ 156.25 and 84.02, respectively. However, they disappeared in the spectra of **3** and **P1a/2b/CO₂**, demonstrating that the monomers were consumed. At the same time, two new peaks at δ 163.6 and 151.1 were readily assignable to the resonances of the two new formed carbonyl carbons of poly(benzoyleneurea)s. Notably, other peaks in the monomers could be found at the

almost same sites in the polymers. The spectra of other polymers were similar, which were provided in Figures S2–S8 and S10–S23. These spectral characterization confirms that MCP of CO₂, isocyanides and 2-iodoanilines was successfully established and poly(benzoyleneurea)s with defined structures were generated.

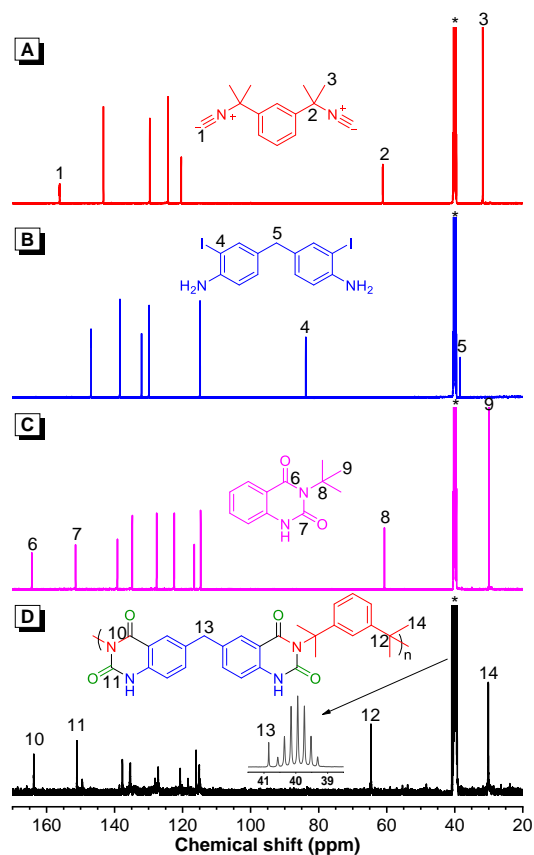


Figure 3. ¹³C NMR spectra of (A) monomer **1a**, (B) monomer **2b**, (C) model compounds **3**, and (D) **P1a/2b/CO₂** in DMSO-*d*₆. The solvent peaks are marked with asterisks.

Self-Assembly Property. Structurally, our resultant poly(benzoyleneurea)s contain two amide groups in one repeating unit, in which the interaction of N–H···O=C hydrogen bonds will facilitate the construction of molecular assemblies.^{43,44} In this regard, the self-assembly properties of poly(benzoyleneurea)s were studied. The results showed that all the polymers could form sphere structures with the volatilization of the solvent of DMF (Figure 4 and Figure S26). And their size

distribution ranges between 200 and 1000 nm. To furnish the self-assemble micro/nano-structure spheres with functionalities, we incorporated a tetraphenylethene (TPE) moiety, a typical unit featuring the aggregation-induced emission (AIE) characteristics, into the polymers to enable them with fluorescence.^{45,46} Thanks to their high polarity, the **2c** and **2d** monomers containing *cis*- and *trans*-TPE could be isolated, from which **P1a/2c/CO₂** and **P1a/2d/CO₂** were prepared (Scheme 1), and the self-assembly during solvent volatilization could be clearly visualized by CLSM (Figure S27). In addition, the **P1a/2c/CO₂** and **P1a/2d/CO₂** showed the unique aggregation-enhanced emission (AEE) features (Figures 5 and S29). For example, **P1a/2c/CO₂** emitted weakly at 496 nm in DMF solution. With the addition of poor solvent of water, the emission enhanced gradually due to the restriction of intramolecular motion of the TPE units and the maximum photoluminescence intensity was recorded in DMF/water mixture with 80% water fraction, which was 3.7-fold higher than that in DMF.

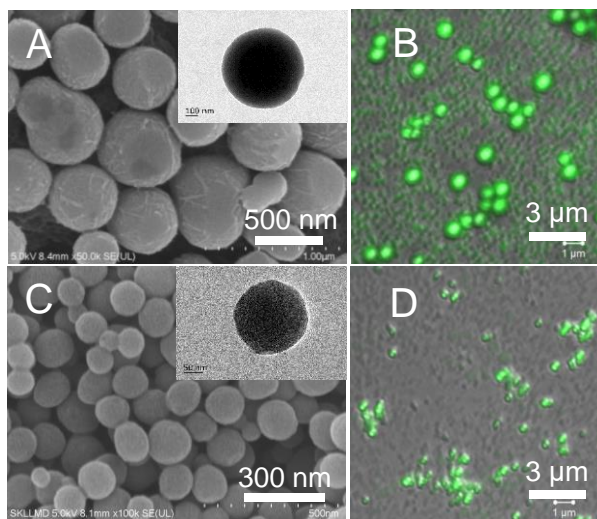


Figure 4. SEM and CLSM images of (A) and (B) **P1a/2c/CO₂**, and (C) and (D) **P1a/2d/CO₂**. The spheres were fabricated by the evaporation of its DMF solutions (concentration: 0.5 mg/mL). Excitation wavelength for the CLSM images: 405 nm. Inset in panels A and C: TEM images.

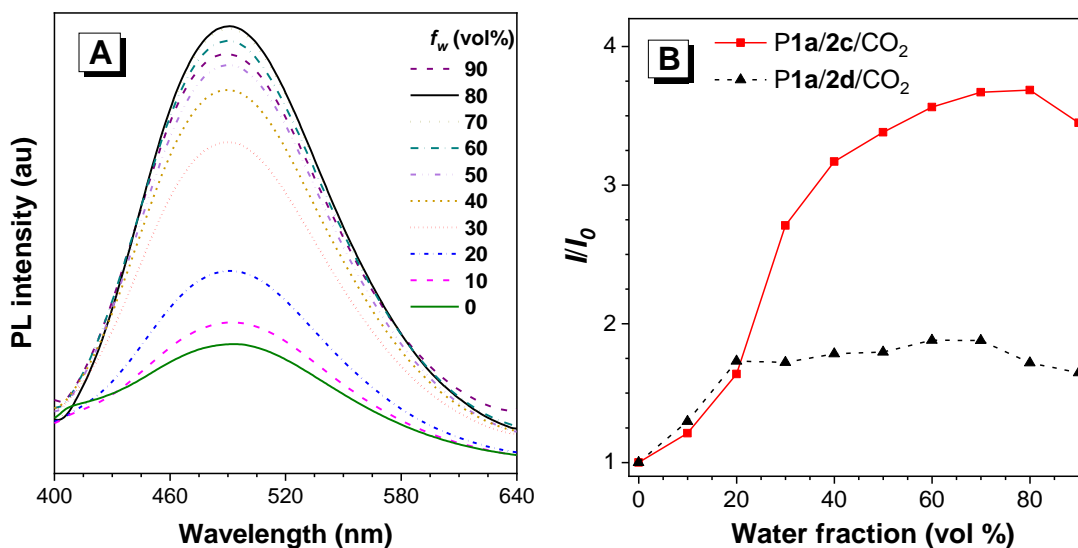


Figure 5. (A) PL spectra of P1a/2c/CO₂ in DMF/water mixtures with different water fractions. Concentration: 10 μ M. λ_{ex} : 340 nm. (B) Plot of relative PL intensity (I/I_0) of P1a/2c/CO₂ and P1a/2d/CO₂ versus water fraction in DMF/water mixtures, where I = the emission peak intensity in the mixtures and I_0 = peak intensity in DMF.

Interestingly, the size of the spheres of the P1a/2c/CO₂ was bigger than that of the P1a/2d/CO₂ (Figure 4). To have a deep insight into the different self-assemble behaviors, the model compounds **4** and **5** were prepared in the yields of 75% and 83%, respectively (Scheme S6, Figures S9, S24 and S25). The single crystals of **4** (CCDC 2013880) and **5** (CCDC 2014002) showed that they manifested a highly twisted conformation (Figure 6A and B) and numerous intermolecular hydrogen binding interactions were observed. As seen in Figure 6C, the N-H \cdots O=C interaction (1.917 \AA) in the *cis*-isomer **4** was stronger than that (1.970 \AA) in *trans*-isomer **5** and the packing of the former was tighter than that of the latter (Figure S28). Thus, the supramolecular interactions of P1a/2c/CO₂ are stronger than those of P1a/2d/CO₂, which could be the reason for the smaller self-assembly sizes of P1a/2d/CO₂.

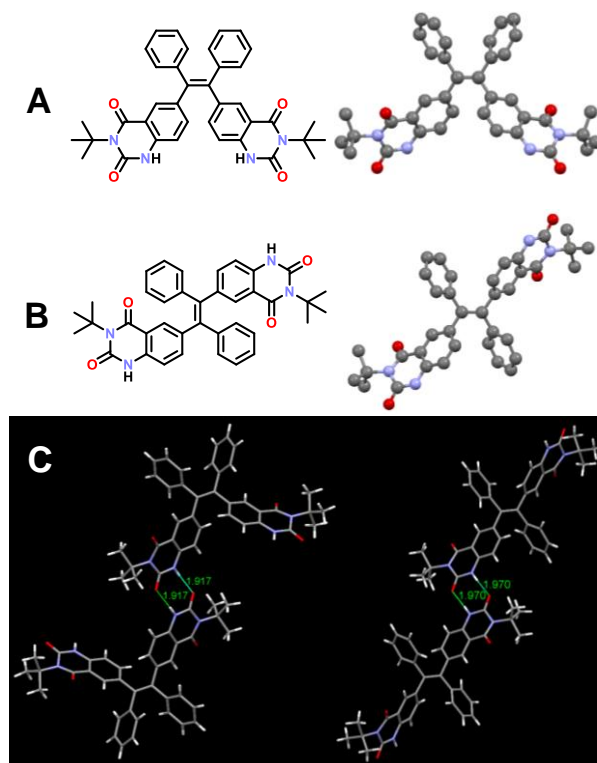


Figure 6. The crystal structures of **4** (A) and **5** (B) and the intermolecular hydrogen bonding interactions in their crystals (C).

Next, we investigated the solvent effect on the self-assembly by taking **P1a/2d**/CO₂ as an example. The assemblies of the polymer could form large connected void net structures in HFIP probably because its polarity is too strong to destroy the intermolecular hydrogen bonding interactions of polymer chains (Figure 7A). While regular and uniform sphere structures were obtained in DMSO, DMF and DMAc (Figure 7B–E). Interestingly, spheres with smaller size could be gained via rapid solution precipitation (Figure 7F). These results suggest that the self-assembly could be fine-tuned through solvent and assembly methods.

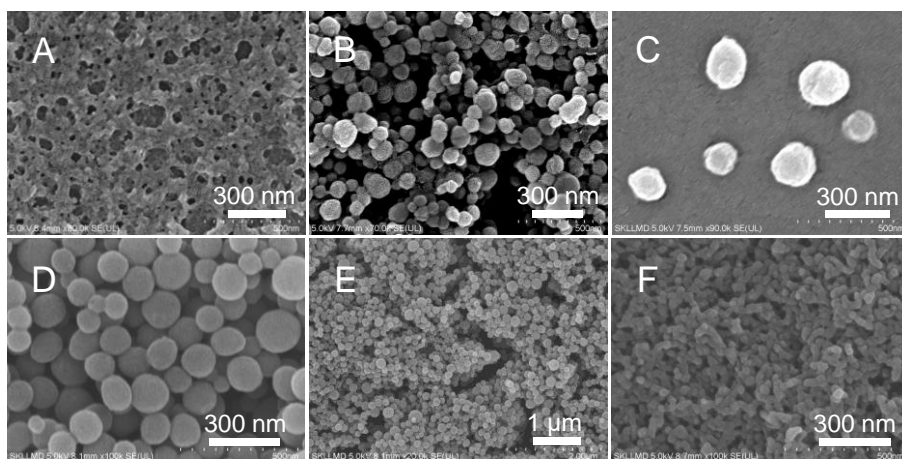


Figure 7. SEM images of P1a/2d/CO₂ on silicon wafers fabricated by direct vaporization of the solutions of (A) HFIP, (B) DMSO, (C) DMAc, (D) and (E) DMF solution (concentration: 0.5 mg/mL) and by (F) fast injection of DMF solution into methanol.

Gold Ion Detection. Thanks to their AEE features and possible coordination effect, P1a/2c/CO₂ and P1a/2d/CO₂ could be applied in detection of Au³⁺ ions. Despite the interesting chemical and medicinal properties of Au³⁺ ions, their soluble salts could cause cell toxicity in living organisms arising from the strong binding with biomolecules such as DNA and enzymes.^{47,48} Based on the widely use in catalysis and the toxicity associated with Au³⁺, it is necessary to develop fluorescent probes with high sensitivity and selectivity for Au³⁺.⁴⁹

First, we investigated the selectivity of P1a/2c/CO₂ for 13 different kinds of metal ions including Au³⁺, Pt⁴⁺, Rh³⁺, Ru³⁺, Zn²⁺, Ni²⁺, Pb²⁺, Cd²⁺, Cu²⁺, Mn²⁺, Co²⁺, Cr³⁺, Ag⁺. As shown in Figure 8, the PL intensity of P1a/2c/CO₂ in DMF/water mixtures with f_w of 80% showed no obvious changes after the addition of other metal ions except a remarkable reduction upon Au³⁺ ions, demonstrating that P1a/2c/CO₂ could selectively detect Au³⁺ ions.

Then, we studied possible sensing mechanism. No new peak occurred in the absorption spectra of the polymer upon gradually adding Au³⁺ ions (Figure S30A). Moreover, the lifetime of the

polymer in the presence of the Au^{3+} ions became shorter (Figure S30B). These results suggest that a dynamic quenching might be occurred. In addition, the PL spectrum of the polymer barely overlapped with the absorption spectrum of Au^{3+} ions (Figure S31). Thus, the PL quenching could be attributed to the coordination interactions of **P1a/2c**/ CO_2 with the Au^{3+} ions by the formation of supramolecular species.⁵⁰

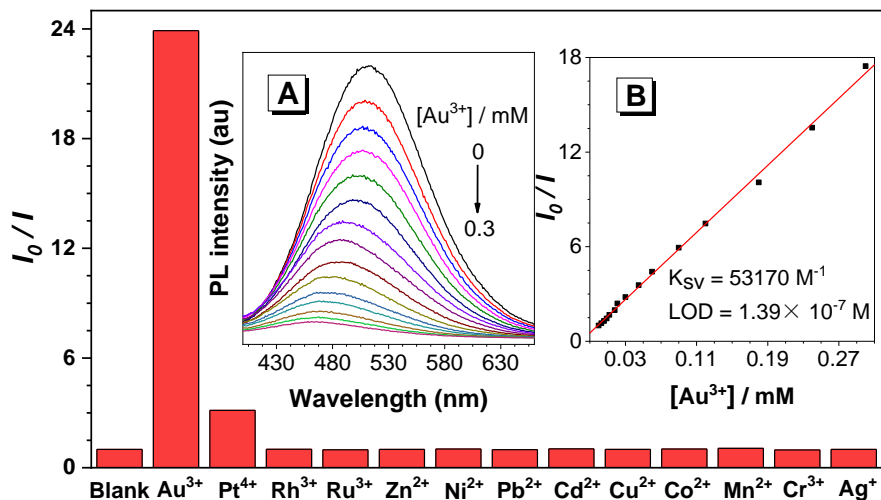


Figure 8. Selective detection of Au^{3+} by **P1a/2c**/ CO_2 in DMF/water mixtures with 80% water fraction among 13 kinds of metal ions. $[\text{P1a/2c/CO}_2] = 10^{-6}$ M, $[\text{Metal ion}] = 5 \times 10^{-5}$ M. Inset: (A) PL spectra of the **P1a/2c**/ CO_2 in DMF/water mixture with f_w of 80% with different Au^{3+} concentrations. λ_{ex} : 340 nm. (B) Stern–Volmer plots of I_0/I of **P1a/2c**/ CO_2 solution versus Au^{3+} concentration, where I = peak intensity and I_0 = peak intensity at $[\text{Au}^{3+}] = 0$.

Another important parameter for a chemosensor is its sensitivity. We then tested the sensitivity of our polymer towards Au^{3+} ions. The PL intensity gradual weakened with the addition of Au^{3+} ions (Figure 8A). When the concentration of Au^{3+} ions was lower than 0.30 mM, the Stern–Volmer plot of **P1a/2c**/ CO_2 showed a linear relationship, from which a quenching constant of 53170 M^{-1} was deduced (Figure 8B). The limit of detection (LOD) was calculated to be 1.39×10^{-7} M (ca. $0.027 \mu\text{g} \cdot \text{mL}^{-1}$), which is far below the Au^{3+} toxicity values ($6\text{--}75 \mu\text{g} \cdot \text{L}^{-1}$) for various aquatic

organisms,⁵¹ indicating its potential application for Au³⁺ detection in aquatic ecosystem. Notable, **P1a/2d**/CO₂ could also be used to detect Au³⁺ ions, but with a higher LOD of 9.49×10^{-7} M (Figure S32 and S33), presumably due to the weaker hydrogen-bonding interaction than **P1a/2c**/CO₂.

Conclusion

In this work, we have successfully developed an efficient three-component polymerization of CO₂, isocyanides and 2-iodoanilines, and soluble and thermally stable poly(benzoyleneurea)s with well-defined structures are constructed under mild reaction conditions for the first time. Thanks to the hydrogen bonding interactions of the formed amide groups, the polymers could self-assemble into spheres with the sizes of 200-1000 nm. Moreover, the TPE-containing polymers show the unique AEE features, enable them to be used to visualize the self-assembly processes and acted as fluorescence probes to selectively and sensitively detected Au³⁺ ions. Thus, this work not only offers a new strategy for CO₂ utilization but also provides perspective for the design and synthesis of heterocyclic polymers from CO₂ and isocyanide.

ASSOCIATED CONTENT

Supporting Information

The supporting information is available free of charge at <https://pubs.acs.org>.

Materials and instruments; details of synthesis; polymerization condition optimization; characterization data (TGA, FT-IR, NMR, UV, PL, SEM, CLSM, etc.)

AUTHOR INFORMATION

Corresponding Author

*E-mail: msqinaj@scut.edu.cn (A.J.Q.);

*E-mail: tangbenz@ust.hk (B.Z.T).

Notes

The authors declare no competing financial interest.

ACKNOWLEDGMENT

This work was financially supported by the National Natural Science Foundation of China (21788102 and 21525417), the Natural Science Foundation of Guangdong Province (2019B030301003 and 2016A030312002), and the Innovation and Technology Commission of Hong Kong (ITCCNERC14S01).

REFERENCES

- (1) Castro, S.; Albo, J.; Irabien, A. Photoelectrochemical Reactors for CO₂ Utilization. *ACS Sustain. Chem. Eng.* **2018**, *6*, 15877-15894.
- (2) Bahari, N. A.; Wan Isahak, W. N. R.; Masdar, M. S.; Yaakob, Z. Clean Hydrogen Generation and Storage Strategies via CO₂ Utilization into Chemicals and Fuels: A Review. *Int. J. Energ. Res.* **2019**, *43*, 5128-5150.
- (3) Zhang, Z.; Pan, S. Y.; Li, H.; Cai, J.; Olabi, A. G.; Anthony, E. J.; Manovic, V. Recent Advances in Carbon Dioxide Utilization. *Renew. Sust. Energ. Rev.* **2020**, *125*, 109799.
- (4) Liu, Q.; Wu, L.; Jackstell, R.; Beller, M. Using Carbon Dioxide as a Building Block in Organic Synthesis. *Nat. Commun.* **2015**, *6*, 5933.
- (5) Dabral, S.; Schaub, T. The Use of Carbon Dioxide (CO₂) as a Building Block in Organic Synthesis from an Industrial Perspective. *Adv. Synth. Catal.* **2019**, *361*, 223-246.
- (6) Wang, J.; Qin, A.; Tang, B. Z. Multicomponent Polymerizations Involving Green Monomers. *Macromol. Rapid Commun.* **2020**, *53*, 2516–2525.

- (7) Huang, K.; Sun, C. L.; Shi, Z. J. Transition-Metal-Catalyzed C-C Bond Formation through the Fixation of Carbon Dioxide. *Chem. Soc. Rev.* **2011**, *40*, 2435-2452.
- (8) Cokoja, M.; Bruckmeier, C.; Rieger, B.; Herrmann, W. A.; Kuhn, F. E. Transformation of Carbon Dioxide with Homogeneous Transition-Metal Catalysts: A Molecular Solution to a Global Challenge? *Angew. Chem. Int. Ed.* **2011**, *50*, 8510-8537.
- (9) Cherubini-Celli, A.; Mateos, J.; Bonchio, M.; Dell'Amico, L.; Companyo, X. Transition Metal-Free CO₂ Fixation into New Carbon-Carbon Bonds. *ChemSusChem* **2018**, *11*, 3056-3070.
- (10) Yang, Z. Z.; He, L. N.; Gao, J.; Liu, A. H.; Yu, B. Carbon Dioxide Utilization with C–N Bond Formation: Carbon Dioxide Capture and Subsequent Conversion. *Energ. Environ. Sci.* **2012**, *5*, 6602-6639.
- (11) Chen, Z.; Hadjichristidis, N.; Feng, X.; Gnanou, Y. Cs₂CO₃-Promoted Polycondensation of CO₂ with Diols and Dihalides for the Synthesis of Miscellaneous Polycarbonates. *Polym. Chem.* **2016**, *7*, 4944-4952.
- (12) Chen, Z.; Hadjichristidis, N.; Feng, X.; Gnanou, Y. Poly(urethane–carbonate)s from Carbon Dioxide. *Macromolecules* **2017**, *50*, 2320-2328.
- (13) Li, Y.; Zhang, Y. Y.; Hu, L. F.; Zhang, X. H.; Du, B. Y.; Xu, J. T. Carbon Dioxide-Based Copolymers with Various Architectures. *Prog. Polym. Sci.* **2018**, *82*, 120-157.
- (14) Song, B.; He, B.; Qin, A.; Tang, B. Z. Direct Polymerization of Carbon Dioxide, Dienes, and Alkyl Dihalides under Mild Reaction Conditions. *Macromolecules* **2017**, *51*, 42-48.
- (15) Wu, P. X.; Cheng, H. Y.; Shi, R. H.; Jiang, S.; Wu, Q. F.; Zhang, C.; Arai, M.; Zhao, F. Y. Synthesis of Polyurea via the Addition of Carbon Dioxide to a Diamine Catalyzed by Organic and Inorganic Bases. *Adv. Synth. Catal.* **2019**, *361*, 317-325.

- (16) Song, B.; Qin, A. J.; Tang, B. Z. Green Monomer of CO₂ and Alkyne-Based Four-Component Tandem Polymerization toward Regio- and Stereoregular Poly(aminoacrylate)s. *Chinese J. Polym. Sci.* **2020**, *39*, 51-59.
- (17) Song, B.; Zhang, R.; Hu, R.; Chen, X.; Liu, D.; Guo, J.; Xu, X.; Qin, A.; Tang, B. Z. Site-Selective, Multistep Functionalizations of CO₂-Based Hyperbranched Poly(alkynoate)s toward Functional Polymeric Materials. *Adv. Sci.* **2020**, *7*, 2000465.
- (18) Grignard, B.; Gennen, S.; Jerome, C.; Kleij, A. W.; Detrembleur, C. Advances in the Use of CO₂ as a Renewable Feedstock for the Synthesis of Polymers. *Chem. Soc. Rev.* **2019**, *48*, 4466-4514.
- (19) Song, B, Qin A, Tang B Z. New Polymerizations Based on Green Monomer of Carbon Dioxide. *Acta Chim. Sin.* **2020**, *78*, 9-22.
- (20) Nakano, R.; Ito, S.; Nozaki, K. Copolymerization of Carbon Dioxide and Butadiene via a Lactone Intermediate. *Nat. Chem.* **2014**, *6*, 325-331.
- (21) Liu, M.; Sun, Y.; Liang, Y.; Lin, B. L. Highly Efficient Synthesis of Functionalizable Polymers from a CO₂/1,3-Butadiene-Derived Lactone. *ACS Macro Lett.* **2017**, *6*, 1373-1378.
- (22) Zhang, Y.; Xia, J.; Song, J.; Zhang, J.; Ni, X.; Jian, Z. Combination of Ethylene, 1,3-Butadiene, and Carbon Dioxide into Ester-Functionalized Polyethylenes via Palladium-Catalyzed Coupling and Insertion Polymerization. *Macromolecules* **2019**, *52*, 2504-2512.
- (23) Gennen, S.; Grignard, B.; Tassaing, T.; Jérôme, C.; Detrembleur, C. CO₂-Sourced α -Alkylidene Cyclic Carbonates: A Step Forward in the Quest for Functional Regioregular Poly(urethane)s and Poly(carbonate)s. *Angew. Chem. Int. Ed.* **2017**, *56*, 10394-10398.
- (24) Ouhib, F.; Grignard, B.; Van Den Broeck, E.; Luxen, A.; Robeyns, K.; Van Speybroeck, V.; Jerome, C.; Detrembleur, C. A Switchable Domino Process for the Construction of Novel CO₂-

Sourced Sulfur-Containing Building Blocks and Polymers. *Angew. Chem. Int. Ed.* **2019**, *58*, 11768-11773.

(25) Tsuda, T.; Maruta, K.; Kitaike, Y. Nickel(0)-Catalyzed Alternating Copolymerization of Carbon Dioxide with Diynes to Poly(2-pyrones). *J. Am. Chem. Soc.* **1992**, *114*, 1498-1499.

(26) Tsuda, T.; Maruta, K. Nickel(0)-Catalyzed Alternating Copolymerization of 2,6-Octadiyne with Carbon Dioxide to Poly(2-pyrone). *Macromolecules* **1992**, *25*, 6102-6105.

(27) Teffahi, D.; Hocine, S.; Li, C. J. Synthesis of Oxazolidinones, Dioxazolidinone and Polyoxazolidinone (a New Polyurethane) via a Multi Component-Coupling of Aldehyde, Diamine Dihydrochloride, Terminal Alkyne and CO₂. *Lett. Org. Chem.* **2012**, *9*, 585-593.

(28) Fu, W.; Dong, L.; Shi, J.; Tong, B.; Cai, Z.; Zhi, J.; Dong, Y. Multicomponent Spiropolymerization of Diisocyanides, Alkynes and Carbon Dioxide for Constructing 1,6-Dioxospiro[4,4]nonane-3,8-diene as Structural Units under One-Pot Catalyst-Free Conditions. *Polym. Chem.* **2018**, *9*, 5543-5550.

(29) Song, B.; Bai, T.; Xu, X.; Chen, X.; Liu, D.; Guo, J.; Qin, A.; Ling, J.; Tang, B. Z. Multifunctional Linear and Hyperbranched Five-Membered Cyclic Carbonate-Based Polymers Directly Generated from CO₂ and Alkyne-Based Three-Component Polymerization. *Macromolecules* **2019**, *52*, 5546-5554.

(30) Lygin, A. V.; de Meijere, A. Isocyanides in the Synthesis of Nitrogen Heterocycles. *Angew. Chem. Int. Ed.* **2010**, *49*, 9094-9124.

(31) Kruithof, A.; Ruijter, E.; Orru, R. V. Synthesis of Heterocycles by Formal Cycloadditions of Isocyanides. *Chem. Asian J.* **2015**, *10*, 508-520.

- (32) Nair, V.; Rajesh, C.; Vinod, A. U.; Bindu, S.; Sreekanth, A. R.; Mathen, J. S.; Balagopal, L. Strategies for Heterocyclic Construction via Novel Multicomponent Reactions Based on Isocyanides and Nucleophilic Carbenes. *Acc. Chem. Res.* **2003**, *36*, 899-907.
- (33) Jiang, B.; Rajale, T.; Wever, W.; Tu, S. J.; Li, G. Multicomponent Reactions for the Synthesis of Heterocycles. *Chem. Asian J.* **2010**, *5*, 2318-2335.
- (34) Varadi, A.; Palmer, T. C.; Notis Dardashti, R.; Majumdar, S. Isocyanide-Based Multicomponent Reactions for the Synthesis of Heterocycles. *Molecules* **2015**, *21*, 19.
- (35) Mampuy, P.; Neumann, H.; Sergeyev, S.; Orru, R. V. A.; Jiao, H.; Spannenberg, A.; Maes, B. U. W.; Beller, M. Combining Isocyanides with Carbon Dioxide in Palladium-Catalyzed Heterocycle Synthesis: N3-Substituted Quinazoline-2,4(1H,3H)-Diones via a Three-Component Reaction. *ACS Catal.* **2017**, *7*, 5549-5556.
- (36) Xu, P.; Wang, F.; Wei, T. Q.; Yin, L.; Wang, S. Y.; Ji, S. J. Palladium-Catalyzed Incorporation of Two C1 Building Blocks: The Reaction of Atmospheric CO₂ and Isocyanides with 2-Iodoanilines Leading to the Synthesis of Quinazoline-2,4(1H,3H)-Diones. *Org. Lett.* **2017**, *19*, 4484-4487.
- (37) Zhang, W. Z.; Li, H.; Zeng, Y.; Tao, X.; Lu, X. Palladium-Catalyzed Cyclization Reaction of O-Haloanilines, CO₂ and Isocyanides: Access to Quinazoline-2,4(1H,3H)-Diones. *Chin. J. Chem.* **2018**, *36*, 112-118.
- (38) Dahlenburg, L.; Treffert, H.; Heinemann, F. W. 1,3-Bis(α -aminoisopropyl)benzene, *Meta*-C₆H₄(CMe₂NH₂)₂: An *N,N*-Bridging and *N,C,N*-Cyclometalating Ligand. *Inorg. Chim. Acta.* **2008**, *361*, 1311-1318.

- (39) Tian, T.; Hu, R.; Tang, B. Z. Room Temperature One-Step Conversion from Elemental Sulfur to Functional Polythioureas through Catalyst-Free Multicomponent Polymerizations. *J. Am. Chem. Soc.* **2018**, *140*, 6156-6163.
- (40) Hill, N. L.; Braslau, R. Synthesis and Characterization of a Novel Bisnitroxide Initiator for Effecting “Outside-In” Polymerization. *Macromolecules* **2005**, *38*, 9066-9074.
- (41) Sunke, R.; Kumar, V.; Ashfaq, M. A.; Yellanki, S.; Mediseti, R.; Kulkarni, P.; Ramarao, E. V. V. S.; Ehtesham, N. Z.; Pal, M. A Pd(II)-Catalyzed C–H Activation Approach to Densely Functionalized N-Heteroaromatics Related to Neocryptolepine and Their Evaluation as Potential Inducers of Apoptosis. *RSC Adv.* **2015**, *5*, 44722-44727.
- (42) Peng, X.; Zhu, L.; Hou, Y.; Pang, Y.; Li, Y.; Fu, J.; Yang, L.; Lin, B.; Liu, Y.; Cheng, M. Access to Benzo[*a*]carbazoles and Indeno[1,2-*c*]quinolines by a Gold(I)-Catalyzed Tunable Domino Cyclization of Difunctional 1,2-Diphenylethyne. *Org. Lett.* **2017**, *19*, 3402-3405.
- (43) Seo, M.; Park, J.; Kim, S. Y. Self-Assembly Driven by an Aromatic Primary Amide Motif. *Org. Biomol. Chem.* **2012**, *10*, 5332-5342.
- (44) Sherrington, D. C.; Taskinen, K. A. Self-Assembly in Synthetic Macromolecular Systems via Multiple Hydrogen Bonding Interactions. *Chem. Soc. Rev.* **2001**, *30*, 83-93.
- (45) Feng H. T.; Lam J. W. Y.; Tang B. Z. Self-Assembly of AIEgens. *Coord. Chem. Rev.* **2020**, *406*, 213142.
- (46) Lou X. Y.; Yang Y. W. Aggregation-Induced Emission Systems involving Supramolecular Assembly. *Aggregate* **2020**, *1*, 19-30.
- (47) Lee, M. T.; Ahmed, T.; Friedman, M. E. Inhibition of Hydrolytic Enzymes by Gold Compounds. I. Beta-Glucuronidase and Acid Phosphatase by Sodium Tetrachloroaurate (III) and Potassium Tetrabromoaurate (III). *J. Enzym. Inhib.* **1989**, *3*, 23-33.

(48) Nyarko, E.; Hara, T.; Grab, D. J.; Habib, A.; Kim, Y.; Nikolskaia, O.; Fukuma, T.; Tabata, M. In Vitro Toxicity of Palladium(II) and Gold(III) Porphyrins and Their Aqueous Metal Ion Counterparts on Trypanosoma Brucei Brucei Growth. *Chem. Biol. Interact.* **2004**, *148*, 19-25.

(49) Zhang, J. F.; Zhou, Y.; Yoon, J.; Kim, J. S. Recent Progress in Fluorescent and Colorimetric Chemosensors for Detection of Precious Metal Ions (Silver, Gold and Platinum Ions). *Chem. Soc. Rev.* **2011**, *40*, 3416-3429.

(50) Doidge, E. D.; Carson, I.; Tasker, P. A.; Ellis, R. J.; Morrison, C. A.; Love, J. B. A Simple Primary Amide for the Selective Recovery of Gold from Secondary Resources. *Angew. Chem. Int. Ed.* **2016**, *55*, 12436-12439.

(51) Nam, S. H.; Lee, W. M.; Shin, Y. J.; Yoon, S. J.; Kim, S. W.; Kwak, J. I.; An, Y. J. Derivation of Guideline Values for Gold (III) Ion Toxicity Limits to Protect Aquatic Ecosystems. *Water Res.* **2014**, *48*, 126-136.

Table of Contents

